THE JOURNAL OF BIOLOGICAL CHEMISTRY
Vol. 276, No. 50, Issue of December 14, pp. 47311–47319, 2001
Printed in U.S.A.

Acquisition of a Specific and Potent PTP1B Inhibitor from a Novel Combinatorial Library and Screening Procedure*

Received for publication, July 12, 2001, and in revised form, September 28, 2001
Published, JBC Papers in Press, October 2, 2001, DOI 10.1074/jbc.M106568200

Kui Shen‡§, Yen-Fang Keng§¶, Li Wu¶, Xiao-Ling Guo¶, David S. Lawrence‡‖, and Zhong-Yin Zhang‡¶**

From the Departments of ‡Biochemistry and ¶Molecular Pharmacology, Albert Einstein College of Medicine, Yeshiva University, Bronx, New York 10461

Protein-tyrosine phosphatases (PTPases) form a large family of enzymes that serve as key regulatory components in signal transduction pathways. Defective or inappropriate regulation of PTPase activity leads to aberrant tyrosine phosphorylation, which contributes to the development of many human diseases including cancers and diabetes. For example, recent gene knockout studies in mice identify PTP1B as a promising target for anti-diabetes/obesity drug discovery. Thus, there is intense interest in obtaining specific and potent PTPase inhibitors for biological studies and pharmacological development. However, given the highly conserved nature of the PTPase active site, it is unclear whether selectivity in PTPase inhibition can be achieved. We describe a combinatorial approach that is designed to target both the active site and a unique peripheral site in PTP1B. Compounds that can simultaneously associate with both sites are expected to exhibit enhanced affinity and specificity. We also describe a novel affinity-based high-throughput assay procedure that can be used for PTPase inhibitor screening. The combinatorial library/high-throughput screen protocols furnished a small molecule PTP1B inhibitor that is both potent (K_i = 2.4 nM) and selective (little or no activity against a panel of phosphatases including *Yersinia* PTPase, SHP1, SHP2, LAR, HePTP, PTPα, CD45, VHR, MKP3, Cdc25A, Stp1, and PP2C). These results demonstrate that it is possible to acquire potent, yet highly selective inhibitors for individual members of the large PTPase family of enzymes.

The initiation, propagation, and termination of signaling events controlling many cellular processes are determined by the level of tyrosine phosphorylation. Phosphotyrosine level, in turn, is maintained in an exquisite balance by the reciprocal activities of protein-tyrosine kinases and protein-tyrosine phosphatases (PTPases).[1] To date, a large number of PTPases have been identified. Because balanced protein-tyrosine phosphorylation is critical for the maintenance of cellular homeostasis, it is not surprising that PTPase malfunction has been linked to many human diseases (1). Consequently, in those instances where PTPase activity is inappropriately high, PTPase inhibitors may provide a valuable new family of therapeutic agents. However, drug development targeted to PTPases was not seriously considered until recently. A major concern is that a PTPase may regulate multiple signaling pathways, whereas, at the same time, a single pathway may be controlled by several PTPases. Thus, PTPase inhibition may give rise to unwanted side effects. Significant progress has been made that is beginning to alleviate this concern.

For example, PTP1B has been suggested as a negative regulator of insulin signaling (2–4). In addition to a role in insulin signaling, PTP1B is overexpressed in association with the expression of $p185^{c\text{-}erbB\text{-}2}$ in human breast and ovarian cancers (5, 6), and PTP1B is capable of suppressing transformation by Neu (7) and v-Src (8). Recently, PTP1B has been identified as the major PTPase that dephosphorylates and activates c-Src in several human breast cancer cell lines (9). PTP1B is also capable of antagonizing signaling by the epidermal growth factor receptor (10, 11) and the oncoprotein $p210^{bcr\text{-}abl}$ (12) by directly dephosphorylating the epidermal growth factor receptor and the $p210^{bcr\text{-}abl}$ tyrosine kinase. Furthermore, PTP1B can negatively regulate integrin-mediated adhesion and signaling by binding and dephosphorylating β-catenin (13) and $p130^{cas}$ (Crk-associated substrate) (14). Interestingly, other potential substrates for PTP1B include the prolactin-activated signal transducers and activators of transcription STAT5a and STAT5b (15).

The results described above, taken together, suggest that PTP1B may be a participant in several signaling pathways. Thus, PTP1B might not be considered as an ideal target for drug development. However, $PTP1B^{-/-}$ mice display increased insulin receptor and insulin receptor substrate-1 phosphorylation and enhanced sensitivity to insulin in skeletal muscle and liver (16, 17). In addition, $PTP1B^{-/-}$ mice have remarkably low adiposity and are protected from diet-induced obesity. Perhaps

* This work was supported in part by National Institutes of Health Grant GM55242. The costs of publication of this article were defrayed in part by the payment of page charges. This article must therefore be hereby marked "*advertisement*" in accordance with 18 U.S.C. Section 1734 solely to indicate this fact.

§ These two authors contributed equally to this work.

‖ To whom correspondence may be addressed: Dept. of Biochemistry, Albert Einstein College of Medicine, Yeshiva University, 1300 Morris Park Ave., Bronx, NY 10461. Tel.: 718-430-8641; E-mail: dlawrenc@aecom.yu.edu.

** Irma T. Hirschl career scientist. To whom correspondence may be addressed: Dept. of Molecular Pharmacology, Albert Einstein College of Medicine, Yeshiva University, 1300 Morris Park Ave., Bronx, NY 10461. Tel.: 718-430-4288; E-mail: zyzhang@aecom.yu.edu.

[1] The abbreviations used are: PTPase, protein-tyrosine phosphatase; Boc, *tert*-butoxylcarbonyl; BSA, bovine serum albumin; DMA, *N,N*-dimethylacetamide; DMF, *N,N*-dimethylformamide; DMG, 3,3-dimethyl glutarate; DTT, dithiothreitol; ELISA, enzyme-linked immunosorbent assay; ESI-MS, electron spray ionization-mass spectroscopy; Fmoc, 9-fluorenylmethoxycarbonyl; Fmoc-Osu, *N*-(9-fluorenylmethoxycarbonyloxy)succinimide; F_2Pmp, phosphonodifluoromethyl phenylalanine; GST, glutathione *S*-transferase; HBTU, 2-(1H-benzotriazol-1-yl)-1,1,3,3-tetramethyluronium hexafluorophosphate; HPLC, high performance liquid chromatography; HOBt, *N*-hydroxybenzotriazole; MALDI-TOF, matrix-assisted laser desorption ionization-time of flight; MS, mass spectroscopy; NMM, *N*-methylmorpholine; PBS, phosphate-buffered saline; *p*NPP, *p*-nitrophenyl phosphate; TCPTP, T cell PTPase; THF, tetrahydrofuran; Tyr(P), *O*-phospho-L-tyrosine.

most importantly, these mice appeared to be normal and healthy, indicating that regulation of insulin signaling by PTP1B is tissue- and cell type-specific. These observations suggest that specific PTP1B inhibitors might be free of side effects and highlight the potential of selective therapeutic efficacy in targeting PTP1B (anti-diabetes/obesity) even though PTP1B is expressed ubiquitously. As expected, interest in the development of PTPase-based therapeutics has recently intensified.

Clearly, however, potent and selective PTPase inhibitors are required before therapeutic intervention with PTPase inhibitors can become a reality. Structural and mutational studies have shown that amino acids involved in catalysis or formation of the Tyr(P) binding site (the active site) are conserved (18–20), indicating that PTPases utilize similar mechanisms for phosphomonoester hydrolysis and Tyr(P) recognition. Can specificity be achieved by targeting the PTPase active site for inhibitor development? A similar question was raised in the protein kinase field because of the structural conservation of the ATP binding site. Despite the latter, a number of highly selective, ATP-binding site-targeted, protein kinase inhibitors have been described (21, 22). In several instances, structural studies reveal that specificity comes from the fact that only a portion of each inhibitor interacts with the residues that bind ATP, whereas the rest of the molecule makes contact with residues situated outside the ATP-binding pocket (22).

Kinetic studies of PTPases with Tyr(P)-containing peptides showed that Tyr(P) alone is not sufficient for high affinity binding and residues surrounding the Tyr(P) contribute to efficient substrate recognition (23, 24). This suggests that there are subpockets bordering the active site that can be targeted to enhance inhibitor affinity and selectivity. Furthermore, the Tyr(P)-binding site in PTPases is obviously smaller than the ATP site in protein kinases. Thus, for PTPase inhibitor design, it is critical to consider adjacent peripheral sites in addition to the active site to gain potency and selectivity. In this paper, we describe the construction of a novel combinatorial library designed to target both the active site and an adjacent peripheral site in PTP1B. We also describe the development of an ELISA-based affinity selection procedure that was used to screen for potent PTP1B ligands. We have identified a highly potent PTP1B inhibitor (with a K_i value of 2.4 nM) that exhibits several orders of magnitude selectivity in favor of PTP1B against a panel of PTPases. Our results demonstrate that it is feasible to achieve potency and selectivity for PTPase inhibition.

MATERIALS AND METHODS

General Procedures—All moisture-sensitive reactions were carried out in oven-dried glassware under a positive pressure of dry N_2 or Ar. DMA, DMF, Me_2SO, lithium bis(trimethylsilyl)amide, CH_2Cl_2, and THF for moisture-sensitive reactions were purchased from Aldrich in Sure/Seal™ bottles. All reactions were followed by thin layer chromatography using E. Merck silica gel 60 F-254. Flash column chromatography was performed using J.T. Baker silica gel (230–400 mesh). Benzotriazole-1-yl-oxy-*tris*-(dimethylamino)-phosphonium hexafluorophosphate, 1,3-diisopropylcarbodiimide, HBTU, HOBt, piperidine, benzotriazole-1-yl-oxy-*tris*-pyrrolidino-phosphonium hexafluorophosphate, tetramethylfluoroformamidinium hexafluorophosphate, and *O*-(*N*-succinimidyl)-1,1,3,3-tetramethyluronium tetrafluoroborate for peptide synthesis were purchased from Advanced ChemTech. The structures of new compounds were characterized by ^{1}H NMR (300 MHz), ^{13}C NMR (75.5 MHz), ^{19}F NMR (282 MHz), and ^{31}P NMR (121 MHz) at 299 K unless otherwise indicated, and by ESI-MS analysis.

Peptide Synthesis—Peptides (biotinyl-caproic acid-DADEpYL-amide and 7-hydroxycoumarin-caproic acid-DADEpYL-amide) were synthesized on Rink amide resin (Advanced ChemTech) using a standard protocol for HBTU/HOBt/NMM activation of Fmoc-protected amino acid derivatives (Advanced ChemTech or Novabiochem). 7-Hydroxycoumarin-4-acetic acid and biotin (Aldrich) were activated with 1.5 eq of *O*-(*N*-succinimidyl)-1,1,3,3-tetramethyluronium tetrafluoroborate and 4 eq of *N,N*-diisopropylethylamine in DMF. Side chains of Asp and Glu were *tert*-butyl-protected; the phosphate group of Tyr(P) was mono-benzyl ester-protected. The coupling reaction was performed in DMF for 1.5 h using a 3-fold excess of acid relative to resin-bound amine. Fmoc removal was performed with 20% piperidine in DMF. Final cleavage and side chain deprotection was achieved with 95% trifluoroacetic acid and 2.5% triisopropylsilane in water for 2 h. The resin was removed by filtration, and the remaining solution concentrated. Dry diethyl ether was added and the precipitated peptides collected by centrifugation. The peptides were resuspended, washed twice with ether, dissolved in water, and purified by semipreparative reverse phase HPLC. All peptides were obtained in high purity (>95%) as analyzed by MALDI-TOF MS and analytical HPLC.

Synthesis of PTP1B Ligand Library—The library was synthesized on a cystamine-modified Tentagel S NH_2 resin **1** using Fmoc chemistry (25). Tyr(P) was attached to the amino terminus of the resin-linked cystamine (8 g). After Fmoc removal by two 5-min treatments with 30% piperidine in DMF, the resin was washed with DMF, CH_2Cl_2, isopropanol, and ether, and then the residual solvent removed *in vacuo*. The resin was distributed in 220-mg quantities into 20-ml polypropylene filtration tubes (Supelco) for coupling of the next component. The linking diversity elements **4–25** (Fig. 2) were incorporated (except for the absence of a diversity element **26**) into the library in the Fmoc-protected form, which were either commercially available or prepared by treatment of commercially available amino acids with Fmoc-Osu in 1:1 THF and 10% Na_2CO_3. Coupling was accomplished by one 2-h treatment and one 15-h treatment with 6 eq of the amino acid, 6 eq of benzotriazole-1-yl-oxy-*tris*-pyrrolidino-phosphonium hexafluorophosphate, 6 eq of HOBt, and 12 eq of NMM in 4 ml of DMF. The phosphate group of Tyr(P) used in the library synthesis was mono-benzyl ester-protected, and the acid side chains of Asp and Glu *t*-butyl ester-protected. The N-terminal Fmoc group was deprotected by two 5-min treatments with 30% piperidine in DMF. The resin was then washed with DMF, CH_2Cl_2, isopropanol, and ether, and the residual solvent removed *in vacuo*. The coupling and deprotection steps were monitored by examination of free amine substitution level or Fmoc release during the course of the library synthesis until the coupling of the terminal diversity elements. The resin from each filtration tube was then distributed in 5.0-mg quantities into 8 wells in one line of the 96-well synthesis block. The terminal diversity elements **A–H** (Fig. 1) were incorporated into the library by one 2-h and one 15-h coupling using 6 eq of the acid, 6 eq of tetramethylfluoroformamidinium hexafluorophosphate, and 12 eq of *N,N*-diisopropylethylamine in 500 μl of DMF. Those acids containing the phenyl phosphate group were prepared from the carboxyl methyl ester of the corresponding phenol via treatment with phosphoryl chloride in pyridine (26), followed by basic hydrolysis. 2,2′-bipyridine-4,4′-diacid was prepared from 4,4′-dimethyl-2,2′-bipyridine (GFS Chemicals) by treatment with $KMnO_4$ in 25% H_2SO_4 (27). Upon completion of the solid-phase assembly, side chain deprotection was accomplished by two 1-h treatments with 90% trifluoroacetic acid and 5% phenol in water. The resulting resin **3** was then washed extensively with CH_2Cl_2, DMF, MeOH, and H_2O before treatment with 10 mM DTT in 500 μl of 50 mM Tris buffer (pH 8.0) for 3 h. Finally the solution phase was filtered into the 96-well receiving plate to afford the spatially separated library members **3** at a concentration of 0.1 mM (assuming complete conversion for each member). Several library members were resynthesized on larger scale using the same procedure in high yield and purity (about 90%) as assessed by HPLC and MALDI-TOF MS analysis. These library members include the structure **3** derived from subunits **A** and **17** (MOLDI-TOF MS calculated for [M] 653, found $[M - H]^-$ 652.8) and structure **3** derived from subunits **C** and **6** (MOLDI-TOF MS calculated for [M] 633, found $[M + H]^+$ 634.2).

Resynthesis of Selected High Affinity PTP1B Ligands—Several high affinity members of the library were selected based on the initial ELISA screening results, and their analogs without a thiol tail were synthesized on Rink resin according to the above peptide synthesis procedure. These compounds were again subjected to the ELISA evaluation, and the highest affinity compound **21B** was synthesized on large scale. ^{1}H NMR (D_2O): δ 7.4–7.2 (m, 8H), 4.76 (dd, J = 6.0 Hz, 7.5 Hz, 1H), 4.68 (dd, J = 5.7 Hz, 9.0 Hz, 1H), 3.66 (s, 2H), 3.27 (dd, J = 5.7 Hz, 14 Hz, 1H), 3.04 (dd, J = 9.0 Hz, 14 Hz, 1H), 2.9 (dd, J = 6.0 Hz, 17 Hz, 1H), 2.7 (dd, J = 7.5 Hz, 17 Hz, 1H); ^{13}C NMR (D_2O): δ 175.8, 174.9, 174.3, 172, 151.2(d), 150.9(d), 132, 130.8, 130.74, 130.72, 121.06(d), 121.86(d), 54, 50, 41, 36, 35; ^{31}P NMR (D_2O): δ −3.01, −3.03; MOLDI-TOF MS calculated for [M] 589, found $[M + H]^+$ 590.

*Synthesis of Benzyl 4-(Bromomethyl)phenylacetate (**28**)*—To a solution of 4-(bromomethyl)phenylacetic acid **27** (1.5 g, 6.55 mmol) in 30 ml

of CH_2Cl_2 was added benzyl alcohol (10 eq, 6.8 ml) and 4-(dimethylamino)pyridine (0.05 eq, 40 mg). The solution was then chilled to 0 °C, and 1,3-diisopropylcarbodiimide (520 μl, 0.5 eq) was added in a dropwise fashion. The mixture was stirred at room temperature for 6 h and then rotary-evaporated to a reduced volume. Flash column chromatography yielded a white solid **28** (1.0 g, 96%). ^{1}H NMR ($CDCl_3$): δ 7.4–7.3 (m, 7H), 7.28 (d, *J* = 7.9 Hz, 2H), 5.1 (s, 2H), 4.5 (s, 2H), 3.7 (s, 2H); ^{13}C NMR ($CDCl_3$): δ 171, 137, 135, 134, 130, 129, 128.7, 128.5, 128.3, 67, 41, 33.

*Synthesis of Benzyl 4-Formylphenylacetate (**29**)*—Silver tetrafluoroborate (28) (2.3 g, 11.8 mmol) was dissolved in dry Me_2SO (10 ml), and a solution of benzyl 4-(bromomethyl)phenylacetate **28** (3.0 g, 9.4 mmol) in dry Me_2SO (10 ml) was slowly added. The mixture was stirred at room temperature for 12 h, and then triethylamine (2 ml) was added. The mixture was kept for additional 15 min and then subjected to CH_2Cl_2/water extraction. The organic phase was concentrated via rotary evaporation and purified by flash column chromatography to afford a white solid **29** (1.96 g, 82%). ^{1}H NMR ($CDCl_3$): δ 10.0 (s, 1H), 7.8 (d, *J* = 8.3 Hz, 2H), 7.5 (d, *J* = 8.3 Hz, 2H), 7.3 (m, 5H), 5.1 (s, 2H), 3.8 (s, 2H); ^{13}C NMR ($CDCl_3$): δ 192, 170, 140, 135.7, 135.6, 130.2, 130.1, 128.8, 128.6, 128.4, 67, 41.

*Synthesis of Benzyl 4-[(Diethylphosphono)hydroxymethyl]phenylacetate (**30**)*—To sodium hydride (77 mg, 3.2 mmol) in 10 ml of THF at −20 °C was added dropwise diethyl phosphite (430 μl, 3.3 mmol). The solution was stirred for 20 min before a solution of benzyl 4-formylphenylacetate **29** (750 mg, 3.0 mmol) in 8 ml of THF was added. The solution was stirred for additional 30 min and the reaction quenched with 10 ml of 5% NH_4Cl solution. The mixture was extracted by 3 × 15-ml ethyl acetate and the organic phase washed with brine, dried over sodium sulfate, filtered, and concentrated by rotary evaporation. Subsequent flash column chromatography furnished a colorless oil **30** (820 mg, yield 71%). ^{1}H NMR ($CDCl_3$): δ 7.4 (dd, *J* = 1.5 Hz, 7.9 Hz, 2H), 7.3–7.2 (m, 7H), 5.1 (s, 2H), 5.0 (d, *J* = 11 Hz, 1H), 4.8 (s, broad, 1H), 4.0 (m, 4H), 3.6 (s, 2H), 1.23 (t, *J* = 7.2 Hz, ^{3}H), 1.19 (t, *J* = 7.2 Hz, ^{3}H); ^{13}C NMR ($CDCl_3$): δ 171(d), 136.9 (d), 135.8, 133.6(d), 129(d), 128.6, 128.2, 128.1, 127(d), 70(d), 67, 63(m), 41, 16(d); ^{31}P NMR ($CDCl_3$): δ 22.6.

*Synthesis of Benzyl 4-[(Diethylphosphono)difluoromethyl]phenylacetate (**31**)*—To a solution of benzyl 4-[(diethylphosphono)hydroxymethyl]phenylacetate **30** (100 mg, 0.26 mmol) in dry CH_2Cl_2 (5 ml), 260 mg of activated MnO_2 (85%, 2.5 mmol) was added in one portion. The mixture was stirred for 24 h and then filtered through acid-washed silica gel. The filtrate was rotary-evaporated and dried *in vacuo* to afford the ketophosphonate intermediate as a colorless oil. Without further purification, the oil was chilled to 0 °C and 1 ml of (diethylamino)sulfur trifluoride (7.5 mmol) added dropwise. The solution was stirred at room temperature for 6 h and then diluted by 10 ml of CH_2Cl_2. The resulting solution was added slowly to 15 ml of saturated Na_2CO_3 solution at 0 °C. The mixture was extracted by 3 × 10-ml CH_2Cl_2 and the combined organic layer washed by brine, dried over sodium sulfate, filtered, concentrated via rotary evaporation, and purified by flash column chromatography to afford **31** (45 mg, 43%). ^{1}H NMR ($CDCl_3$): δ 7.5 (d, *J* = 7.9 Hz, 2H), 7.4–7.2 (m, 7H), 5.1 (s, 2H), 4.2 (m, 4H), 3.7 (s, 2H), 1.3 (t, *J* = 7.2 Hz, 6H); ^{13}C NMR ($CDCl_3$): δ 170, 137, 136, 132 (m), 129, 128.8, 128.7, 128.5, 128.4, 128.3, 128.2, 126(m), 115(m), 67, 65(d), 41, 16(d); ^{31}P NMR ($CDCl_3$): δ 7.5 (t, *J* = 116 Hz).

*Synthesis of 4-(Phosphonodifluoromethylphenylacetic Acid (**32**)*—Benzyl 4-[(diethylphosphono)difluoromethyl]phenylacetate **31** (123 mg, 0.3 mmol) was chilled to 0 °C by ice-water bath, and 1 ml of iodotrimethylsilane (7.0 mmol) was added to the reaction solution, which was subsequently stirred at room temperature overnight. The solution was concentrated by rotary evaporation to an oily residue, dissolved in a mixed solution of 1 ml of acetonitrile, 1 ml of water, and 0.5 ml of trifluoroacetic acid and stirred for 2 h. The solution was then rotary-evaporated to dryness, dissolved in water, and washed by ether. The aqueous solution was subjected to HPLC purification to afford the desired product **32** (28 mg, 35%). ^{1}H NMR (D_2O): δ 7.6 (d, *J* = 7.9 Hz, 2H), 7.4 (d, *J* = 7.9 Hz, 2H), 3.8 (s, 2H); ^{13}C NMR (D_2O): δ 176, 136(d), 133(dt), 129, 126(dt), 120(dt), 40; ^{31}P NMR (D_2O): δ 5.4 (t, *J* = 105 Hz).

*Synthesis of Benzyl (2R,3S)-6-Oxo-2,3-diphenyl-5-(4-iodobenzyl)-4-morpholinecarboxylate (**34**)*—1 M lithium bis(trimethylsilyl)amide in THF (550 μl, 0.55 mmol) was added in a dropwise fashion to a solution of iodobenzyl bromide **33** (149 mg, 0.50 mol), the lactone **34** (213 mg, 0.55 mmol), and hexamethylphosphoramide (1.5 ml) in THF (15 ml) at −78 °C (29). After stirring for 2 h at −78 °C, the mixture was diluted with EtOAc, washed with water and brine, dried over sodium sulfate, filtered, and the solvent removed via rotary evaporation. Flash column chromatography afforded the desired aryl iodide **33** (242 mg, 80%). Two conformers were observed in a ratio of 1:2 at 299 K; ^{1}H NMR ($CDCl_3$): δ major conformer 7.71 (d, *J* = 7.9 Hz, 2H), 7.43–7.03 (m, 11H, overlapping), 6.83 (m, 2H, overlapping), 6.68–6.62 (m, 2H, overlapping), 6.53 (d, *J* = 7.5 Hz, 2H), 5.35–5.25 (m, 2H, overlapping), 5.20–5.03 (m, 2H, overlapping), 4.91 (d, *J* = 3.0 Hz, 1H), 4.51 (d, *J* = 3.0 Hz, 1H), 3.63 (dd, *J* = 6.8 Hz, 14 Hz, 1H), 3.47–3.31 (m, 1H, overlapping), minor conformer 7.63 (d, *J* = 7.9 Hz, 2H), 7.43–7.03 (m, 11H, overlapping), 6.83 (m, 2H, overlapping), 6.72 (d, *J* = 7.5 Hz, 2H), 6.68–6.62 (m, 2H, overlapping), 5.35–5.25 (m, 1H, overlapping),), 5.23 (dd, *J* = 3.4 Hz, 6.8 Hz, 1H),), 5.20–5.03 (m, ^{3}H, overlapping), 4.71 (d, *J* = 3.0 Hz, 1H), 3.47–3.31 (m, 2H, overlapping); ESI-MS calculated for [M] 603, found $[M + H]^+$ 604.

*Synthesis of Benzyl (2R,3S)-6-Oxo-2,3-diphenyl-5-[(4-((diethylphosphono)difluoro-methyl)benzyl)]-4-morpholinecarboxylate (**36**)*—Zinc powder (520 mg, 8 mmol) in DMA (4 ml) was sonicated for 1 h prior to treatment with a solution of diethyl bromodifluorophosphonate (1.42 ml, 8 mmol) in DMA (4 ml) (30). Sonication was continued for an additional 3 h, and then cuprous bromide (1.15 g, 8 mmol) was added in one portion. After 30 min a DMA solution (4 ml) of the aryl iodide **35** (2.40 g, 4 mmol) was added dropwise, and the resulting mixture was stirred for 24 h, diluted with EtOAc, washed with water and brine, dried over sodium sulfate, filtered, and the solvent removed via rotary evaporation. Flash column chromatography afforded the desired alkylated lactone **36** (1.38 g, 52%). Two conformers were observed in a ratio of 3:7 at 299 K; ^{1}H NMR ($CDCl_3$, 299 K): δ major conformer 7.82 (d, *J* = 7.9 Hz, 2H), 7.61–7.23 (m, 11H, overlapping), 7.01 (d, *J* = 7.9 Hz, 2H), 6.83 (d, *J* = 7.9 Hz, 2H), 6.68 (d, *J* = 7.9 Hz, 2H), 5.55–5.43 (m, 1H, overlapping), 5.33–5.17 (m, 2H, overlapping), 5.08 (d, *J* = 3.0 Hz, 1H), 4.61 (d, *J* = 3.0 Hz, 1H), 4.43–4.19 (m, 4H, overlapping), 3.93 (dd, *J* = 6.8 Hz, 14 Hz, 1H), 3.75–3.55 (m, 1H, overlapping), 1.44 (m, 6H, overlapping), minor conformer 7.75 (d, *J* = 7.9 Hz, 2H), 7.61–7.23 (m, 13H, overlapping), 6.88 (d, *J* = 7.9 Hz, 2H), 6.78 (d, *J* = 7.9 Hz, 2H), 5.55–5.43 (m, 1H, overlapping), 5.43 (dd, *J* = 3.4 Hz, 6.8 Hz, 1H), 5.33–5.17 (m, 2H, overlapping), 4.85 (d, *J* = 3.0 Hz, 1H), 4.43–4.19 (m, 4H, overlapping), 3.75–3.55 (m, 2H, overlapping), 1.44 (m, 6H, overlapping); ^{19}F NMR ($CDCl_3$, 299 K): δ major conformer −108.58 (d, *J* = 115 Hz), −108.78 (d, *J* = 115 Hz), minor conformer −108.67 (d, *J* = 115 Hz), −108.83 (d, *J* = 115 Hz); ^{31}P NMR ($CDCl_3$, 299 K): δ 7.2 (t, *J* = 115 Hz). Conformers were not observed at 373 K; ^{1}H NMR (Me_2SO, 373 K): δ 7.5 (d, *J* = 7.9 Hz, 2H), 7.4 (d, *J* = 7.9 Hz, 2H), 7.3–7.0 (m, 11H), 6.9 (d, *J* = 7.2 Hz, 2H), 6.6 (d, *J* = 7.5 Hz, 2H), 5.8 (s, 1H), 5.2 (d, *J* = 3.0 Hz, 1H), 5.1 (dd, *J* = 4.9 Hz, 8.3 Hz, 1H), 5.0 (s, 2H), 4.1 (m, 4H), 3.58 (dd, *J* = 8.3 Hz, 14 Hz, 1H), 3.49 (dd, *J* = 4.9 Hz, 14 Hz, 1H), 1.256 (t, *J* = 7.2 Hz, ^{3}H), 1.250 (t, *J* = 7.2 Hz, ^{3}H); ^{13}C NMR (Me_2SO, 373 K): δ 167, 153, 138, 135.6, 135.4, 134, 129, 127.6, 127.5, 127.1, 126.9, 126.8, 125.8, 125.5(m), 115(m), 78, 67, 62(d), 60, 58, 15(d); ^{19}F NMR (Me_2SO, 373 K): δ −105.9 (d, *J* = 114 Hz), −106.2 (d, *J* = 114 Hz); ^{31}P NMR (Me_2SO, 373 K): δ 6.8 (t, *J* = 114 Hz); ESI-MS calculated for [M] 663, found $[M + H]^+$ 664.

*Synthesis of 4-[Diethylphosphono]difluoromethyl]-L-phenylalanine (**37**)*—The alkylated lactone **36** (31) (478 mg, 0.72 mmol) in a small volume of MeOH was added to a suspension of 10% Pd/C (200 mg) in EtOH (4 ml) and THF (2 ml). The mixture was stirred for 24 h under H_2 atmosphere and then filtered through Celite. The filtrate was rotary-evaporated to dryness, triturated three times with ether, and the residue then placed under vacuum to afford the desired amino acid **37** (252 mg, 100%). ^{1}H NMR (CD_3OD): δ 7.6 (d, *J* = 7.9 Hz, 2H), 7.4 (d, *J* = 7.9 Hz, 2H), 4.2 (m, 5H), 3.3 (dd, *J* = 4.3 Hz, 14 Hz, 1H), 3.2 (dd, *J* = 8.7 Hz, 14 Hz, 1H), 1.326 (t, *J* = 7.2 Hz, ^{3}H), 1.321 (t, *J* = 7.2 Hz, ^{3}H); ^{13}C NMR (CD_3OD): δ 171, 139, 133(m), 131, 128, 117(m), 66(d), 55, 37, 16(d); ^{31}P NMR (CD_3OD): δ 7.1 (t, *J* = 118 Hz).

*Synthesis of N-α-Fmoc-4-(Phosphonodifluoromethyl)-L-phenylalanine (**38**)*—A solution of the amino acid **37** (535 mg, 1.5 mmol) and $NaHCO_3$ (128 mg, 1.5 mmol) in water (5 ml) and dioxane (5 ml) was cooled in an ice bath and then treated with Fmoc-Osu (720 mg, 2.1 mmol) in a small amount of dioxane (31). After stirring for 3 h at room temperature, the mixture was diluted with saturated $NaHCO_3$ (30 ml) and then washed with ether. The aqueous phase was acidified to pH 2 with 6 N HCl and extracted with EtOAc. The extracts were dried over sodium sulfate, filtered, and the solvents removed yielding the Fmoc amino acid **38** as a white solid (870 mg, 100%). The specific optical rotation $[\alpha]_D^{24}$ = 44° (*c* = 0.1 in chloroform) is consistent with previously reported values (31, 32). ^{1}H NMR (Me_2SO): δ 7.9 (d, *J* = 7.2 Hz, 2H), 7.7–7.3 (m, 10H), 4.2–4.0 (m, 8H), 3.1 (dd, *J* = 4.5 Hz, 14 Hz, 1H), 2.9 (dd, *J* = 11 Hz, 14 Hz, 1H), 1.18 (t, *J* = 7.2 Hz, ^{3}H), 1.17 (t, *J* = 7.2 Hz, ^{3}H); ^{13}C NMR ($CDCl_3$): δ 173, 156, 144, 142, 139, 131(m), 130, 128, 127, 126, 125, 120, 115(m), 67, 65(d), 54, 47, 38, 16(d); ^{19}F NMR ($CDCl_3$): δ −109 (d, *J* = 118 Hz); ^{31}P NMR ($CDCl_3$): δ 7.1 (t, *J* = 118 Hz).

*Synthesis of PTP1B Inhibitor Compound **40***—Synthesis was performed on Rink amide resin using a standard protocol for HBTU/HOBt/NMM activation of acids. The coupling reaction was performed in DMF for 1.5 h using a 3-fold excess of acid relative to resin-bound amine. The fully protected Fmoc amino acid **38**, the Fmoc protected Asp (with side chain *tert*-butyl protected), and the free acid **32** were sequentially coupled to the Rink amide resin. Fmoc removal after each coupling was effected with 20% piperidine in DMF. Final cleavage and side chain deprotection was achieved by treatment with 1 M bromotrimethylsilane-thioanisole in trifluoroacetic acid with 5% 1,2-ethanedithiol and 1% *m*-cresol at 0 °C for 5 h and then at room temperature for 16 h. The resin was removed by filtration, and the remaining solution concentrated. The residue was triturated with ether, dissolved in water, and purified by semipreparative reverse phase HPLC to afford the desired compound **40**. ^{1}H NMR (D_2O): δ 7.6 (m, 4H), 7.4 (m, 4H), 4.7 (m, 2H), 3.7 (s, 2H), 3.3 (dd, J = 5.7 Hz, 14 Hz, 1H), 3.1 (dd, J = 9.4 Hz, 14 Hz, 1H), 2.9 (dd, J = 6.0 Hz, 17 Hz, 1H), 2.7 (dd, J = 7.9 Hz, 17 Hz, 1H); ^{13}C NMR (D_2O): δ 175, 174.5, 174.4, 172, 139, 137, 133(m), 129.69, 129.63, 126(m), 115(m), 54, 50, 42, 37, 35; ^{19}F NMR (D_2O): δ −108.58 (d, J = 105 Hz), −108.66 (d, J = 105 Hz); ^{31}P NMR (D_2O): δ 5.36 (t, J = 105 Hz), 5.35 (t, J = 105 Hz); ESI-MS calculated for [M] 657, found $[M - H]^-$ 656, $[M + H]^+$ 658.

Subcloning of PTP1B/C215S to pGex-KG—The coding region for PTP1B/C215S (residues 1–321) from pT7–7/PTP1B/C215S (33) was cleaved with the restriction enzyme *Nde*I and sequentially treated with the Klenow fragment of DNA polymerase I to generate a blunt-ended molecule. The linearized DNA was digested again with restriction enzyme *Eco*RI. The vector pGex-KG was cleaved with restriction enzymes *Sma*I (Blunt-ended) and *Eco*RI (cohesive-ended). The *Nde*I (blunt) to *Eco*RI DNA fragment of pT7–7/PTP1B/C215S containing PTP1B/C215S and the *Sma*I (blunt) to *Eco*RI fragment of pGex-KG encoding resistance to ampicillin were isolated and ligated together.

Protein Expression and Purification of GST-PTP1B and GST-PTP1B/C215S—pGex-KG/PTP1B (or PTP1B/C215S) was used to transform *Escherichia coli* BL21(DE3) by standard methods. Single colony was selected and grown in 10 ml of 2× YT medium containing 100 μg/ml ampicillin overnight with shaking at 37 °C. A 10-ml overnight culture was transferred to 1 liter of 2× YT medium containing 100 μg/ml ampicillin and shaken at 37 °C until the absorbance at 600 nm was between 0.6 and 0.8. Following the addition of isopropyl-1-thio-β-D-galactopyranoside to a final concentration of 0.2 mM, the culture was incubated at 37 °C with shaking for an additional 4 h. The cells were harvested by centrifugation at 5,000 rpm for 5 min, and the bacterial cell pellets were resuspended in 30 ml of PBS buffer (140 mM NaCl, 2.7 mM KCl, 10 mM Na_2HPO_4, 1.8 mM KH_2PO_4, pH 7.4) with 1 mM dithiothreitol, and 1% Triton X-100. The cells were lysed by passage through a French pressure cell press at 1200 p.s.i. twice. Cellular debris was removed by centrifugation at 15,000 rpm for 30 min, and the supernatant was decanted into a 50-ml conical tube, to which 2 ml of 50% slurry of glutathione-Sepharose 4B (Amersham Pharmacia Biotech) equilibrated with PBS buffer was added. After incubating with gentle agitation at 4 °C for 1 h, the matrix was transferred to a column and washed by 10 bed volumes of PBS buffer with 1 mM dithiothreitol and 0.1% Triton X-100 and 5 bed volumes of 50 mM Tris, pH 7.5, and 1 mM dithiothreitol. After the column was left at room temperature for 10 min, the fusion protein was eluted by addition of 1 bed volume of 10 mM reduced glutathione in 50 mM Tris, pH 8.0. The elution and collection steps were repeated five times. The eluents were pooled and concentrated with a Centriprep-30 filtration unit (Amicon) and changed to pH 7.0 buffer containing 50 mM 3′,3′-dimethylglutarate, 1 mM EDTA, 1 mM dithiothreitol, and I = 0.15 M. The purified protein were made to 30% glycerol and stored at −20 °C.

Other Recombinant PTPases—PTP1B (residues 1–321) (33), *Yersinia* PTPase (34), Stp1 (35), VHR (36), and MKP3 (37) were expressed in *E. coli* and purified as described previously. The coding sequence of the catalytic domain (amino acid residues 1–288) of the human T cell PTPase (TCPTP) was a generous gift from Dr. Harry Charbonneau and TCPTP was expressed and purified as described (38). Recombinant HePTP and the catalytic domains of SHP1 and SHP2 were expressed and purified as His_6 fusion proteins. The catalytic domains of PTPα, LAR, and CD45 were expressed and purified as recombinant glutathione *S*-transferase (GST) fusion proteins (39). The intracellular fragment of PTPα, LAR, and CD45 containing both of the PTPase domains was cleaved off the fusion protein as described using thrombin.

An ELISA-based PTP1B Ligand Screening Procedure—To each well of a Neutravidin-coated 96-well microtiter plate was added 100 μl of 10 nM biotinyl-caproic acid-DADEpYL-amide in 50 mM 3,3-dimethyl glutarate, pH 7.0, I = 0.15 M (DMG buffer). After incubation at 4 °C overnight, the plate was rinsed with the DMG buffer three times (200 μl each). Each well was blocked with 100 μl of a solution containing 2% BSA and 0.2% Tween 20 in DMG buffer and shaken for 2 h at room temperature. The wells were then rinsed four times with 200 μl of a solution containing 0.2% BSA, 0.1% Tween 20 in DMG, pH 7.0 buffer (BSA-T-DMG). In each well of a separate, uncoated 96-well plate, a 60-μl solution of the library component (500 nM in BSA-T-DMG) and a 60-μl solution of the GST-PTP1B/C215S fusion protein (0.4 nM in BSA-T-DMG) were mixed and incubated at room temperature for 1 h. Then 100 μl of this mixture was added to each well of the blocked, biotinyl-caproic acid-DADEpYL-amide-treated 96-well plate, and the plate was shaken for 2 h at room temperature. The wells were rinsed four times with 200 μl of a BSA-T-DMG. Polyclonal rabbit anti-GST antibody (100 μl, 100 ng/ml in BSA-T-DMG) was then added to each well and shaken for 1 h at room temperature (or incubated overnight at 4 °C). The wells were washed four times with 200 μl of a BSA-T-DMG solution. To detect the amount of GST-PTP1B/C215S left in the well, horseradish peroxidase-conjugated mouse anti-rabbit antibody (100 μl, 200 ng/ml in BSA-T-DMG) was added to each well and shaken for 1 h at room temperature. The wells were rinsed four times with 200 μl of a BSA-T-DMG and then twice with 300 μl of DMG buffer. 100 μl of peroxidase substrate (I-step Turbo TMB-ELISA, tetramethylbenzidine) was added to each well and incubated for 5–30 min. To stop the peroxidase reaction, 100 μl of 1 M sulfuric acid solution was added to each well and the absorbance was measured at 450 nm with a SpectraMax 340 plate reader.

Determination of K_d Values—The coumarin-labeled Tyr(P)-containing peptide 7-hydroxycoumarin-caproic acid-DADEpYL-amide is highly fluorescent and does not exhibit significant change in fluorescence upon PTP1B binding. Therefore, the K_d value for the binding of 7-hydroxycoumarin-caproic acid-DADEpYL-amide peptide to PTP1B/C215S was determined via equilibrium dialysis as described previously (25). All measurements were performed in 50 mM 3,3-dimethyl glutarate, pH 7.0, I = 0.15 M buffer at 4 °C. Briefly, Slide-A-Lyzer dialysis slide cassettes (Pierce, 10-kDa molecular mass cut-off, 0.1–0.5 ml capacity) were used, which contained 100 nM GST-PTP1B/C215S and 100 nM 7-hydroxycoumarin-caproic acid-DADEpYL-amide. The cassettes (400 μl final volume) were placed in a beaker containing 100 ml of 100 nM 7-hydroxycoumarin-caproic acid-DADEpYL-amide in the same buffer. As a consequence, the concentration of non-PTP1B-bound peptide was held constant in the dialysis slide cassette over the course of the dialysis experiment (16 h). Differences in fluorescence between the solution in the slide cassette and that in the beaker were determined. The excitation wavelength for the coumarin peptide was 325 nm, and the emission was monitored at 460 nm. The K_d value was calculated from Equation 1.

$$K_P = \frac{([E] - [E \cdot P])[P]}{[E \cdot P]} \quad \text{(Eq. 1)}$$

K_P = K_d of 7-hydroxycoumarin-caproic acid-DADEpYL-amide for PTP1B/C215S, [E] = total PTP1B/C215S concentration, [P] = total 7-hydroxycoumarin-caproic acid-DADEpYL-amide concentration, and [E·P] = concentration of 7-hydroxycoumarin-caproic acid-DADEpYL-amide bound to PTP1B/C215S.

A competition-based assay was used to determine the K_d value for the binding of the nonfluorescent compound **21B** to PTP1B/C215S. The cassettes (400 μl final volume) contained 390 nM GST-PTP1B/C215S, 248 nM nonfluorescent high affinity PTP1B ligand **21B**, and 3.97 μM 7-hydroxycoumarin-caproic acid-DADEpYL-amide. The cassettes were placed in a beaker containing 100 ml of 248 nM nonfluorescent high affinity PTP1B ligand **21B** and 3.97 μM 7-hydroxycoumarin-caproic acid-DADEpYL-amide. The K_d for compound **21B** was obtained via competitive displacement of the coumarin derivative using Equation 2 (25).

$$K_L = \frac{K_P \dfrac{[L][E \cdot P]}{[P]}}{[E] - \dfrac{K_P[E \cdot P]}{[P]} - [E \cdot P]} \quad \text{(Eq. 2)}$$

K_L = K_d of **21B** for PTP1B/C215S, K_P = K_d of 7-hydroxycoumarin-caproic acid-DADEpYL-amide for PTP1B/C215S, [E] = total PTP1B/C215S concentration, [P] = total 7-hydroxycoumarin-caproic acid-DADEpYL-amide concentration, [L] = total **21B** concentration, and [E·P] = concentration of 7-hydroxycoumarin-caproic acid-DADEpYL-amide bound to PTP1B/C215S.

Determination of Inhibition Constants (K_i) and IC_{50} Values—The PTPase activity was assayed using *p*-nitrophenyl phosphate (*p*NPP) as a substrate at 25 °C in 50 mM 3,3-dimethylglutarate buffer, pH 7.0,

containing 1 mM EDTA with an ionic strength of 0.15 M adjusted by addition of NaCl. The reaction was initiated by the addition of the enzyme to a reaction mixture (0.2 ml) containing various concentrations of *p*NPP and quenched after 2–3 min by addition of 0.05 ml of 5 N NaOH. The range of substrate concentration used was 0.2–5 K_m. The nonenzymatic hydrolysis of the substrate was corrected by measuring the control without addition of enzyme. After quenching, the amount of product *p*-nitrophenol was determined from the absorbance at 405 nm detected by a Spectra MAX340 microplate spectrophotometer (Molecular Devices) using a molar extinction coefficient of 18,000 M^{-1} cm^{-1}. The Michaelis-Menten kinetic parameters were determined from a direct fit of the velocity *versus* substrate concentration data to Michaelis-Menten equation using the nonlinear regression program KinetAsyst (IntelliKinetics, State College, PA). Inhibition constants for the PTPase inhibitors were determined for PTP1B and TCPTP in the following manner. The initial rate at eight different substrate concentration concentrations (0.2–5 K_m) was measured at three different fixed inhibitor concentrations (26). The inhibition constant was obtained, and the inhibition pattern was evaluated using a direct curve-fitting program KinetAsyst (IntelliKinetics). IC_{50} values for various phosphatases were determined at 2 mM *p*NPP concentration.

RESULTS AND DISCUSSION

As noted in the Introduction, biochemical and genetic studies suggest that PTP1B is a major modulator of insulin sensitivity and fuel metabolism. Thus, PTP1B represents a potential therapeutic target for the treatment of type II diabetes and obesity. Consequently, small molecules designed to inhibit PTP1B not only hold promise as pharmaceutical agents but also could function as probes for elucidating the roles of PTP1B in specific intracellular pathways involved in normal cellular processes. However, given the highly conserved nature of the PTPase active site (*i.e.* Tyr(P) binding site), it has been assumed that it would be difficult to obtain specific inhibitors targeted to the active site of individual PTPases.

Our previous kinetic studies with Tyr(P)-containing peptides and small molecule aryl phosphates showed that Tyr(P) alone is not sufficient for high affinity binding by PTPases and residues surrounding the Tyr(P) contribute to efficient substrate recognition (24, 26, 40–42). In addition, the crystal structure of PTP1B/C215S complexed with low molecular weight nonpeptidic substrates revealed, quite unexpectedly, the presence of a second aryl phosphate-binding site positioned adjacent to the active site (33). This second site lies within a region that is not conserved among PTPases. As a consequence, this unanticipated observation suggested an alternative paradigm for the design of potent and specific PTP1B inhibitors, namely bidentate ligands that bind to both the active site and a unique adjacent peripheral site. In addition to the second aryl phosphate binding pocket, other subsites, positioned within the local vicinity of the active site, may also be conscripted for inhibitor design. For example, structures of PTPase in complex with Tyr(P)-containing peptides and PTPase sequence alignments have suggested that the α1-β1 loop, the β5-β6 loop, the α5-α6 loop, and the WPD loop contain variable residues that may contribute to substrate specificity. Thus, our strategy to develop potent and PTPase-selective inhibitors for individual members of the PTPase family is to tether together two small ligands that are individually targeted to the active site and a unique proximal noncatalytic site. The rationale for the enhanced affinity of bidentate inhibitors is based on the principle of additivity of free energy of binding. The interaction of an inhibitor with two independent sites (*e.g.*, Tyr(P) site and a unique peripheral site) on one PTPase would be expected to confer exquisite specificity, as other PTPases may not possess an identical second site interaction. Below, we describe a combinatorial approach for the identification of a highly potent and selective PTP1B inhibitor that is able to simultaneously occupy both the active site and a unique second site on PTP1B.

Library Design and Construction—Our first generation library was designed to contain two linked motifs, one targeted to the Tyr(P)-binding catalytic site, and the other targeted to a unique adjacent noncatalytic site in PTP1B. Because of the demanding synthetic requirements associated with the preparation of nonhydrolyzable phosphonate analogs (see below), we felt it prudent to prepare a library of synthetically accessible phosphate-based derivatives. Once a high affinity lead from the latter is identified, it can then be converted into an inhibitor by replacing the phosphate moiety with a difluorophosphonate group. Because Tyr(P) is the canonical ligand for PTPase active site, we decided to structurally bias the library with Tyr(P) to direct library members to the active site. A small array of structurally disparate aryl acids (**A–H**) (Fig. 1) were chosen and linked to Tyr(P) to access binding interactions removed from the active site. These aryl acids include three phenylphosphate-containing species (**A–C**), three phenol-containing species (**D–F**), and two additional aromatic species (**G** and **H**). Members of the aryl acid array were separately linked to Tyr(P) either directly (**26**) or via 22 different amino acids (**4–25**) (Fig. 2), which include 9 linear aliphatic species (**4–10**, **15**, **23**), 11 ring-containing species (**11–14**, **16–20**, **24**, and **25**), and 2 natural acidic amino acids (**21** and **22**). Inclusion of hydrophobic and charged amino acids as linkers could potentially provide additional interactions to enhance PTP1B binding. With these substructures, we constructed a small synthetic library of 184 members ((Tyr(P)) 1 × (linkers) 23 × (diversity elements) 8) by solid phase parallel synthesis (Scheme I) using established approaches (see "Materials and Methods" and references therein).

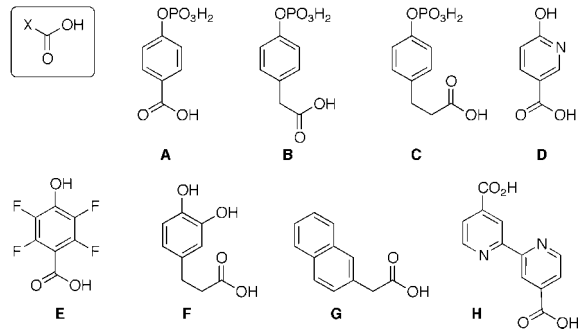

FIG. 1. **Terminal diversity elements used in the library of the general structure 3 to target a unique peripheral site.**

The library was synthesized on a disulfide-modified TentaGel S NH_2 resin **1** using Fmoc chemistry (25). The disulfide linkage between the peptide and the TentaGel resin is stable to the conditions of Fmoc-based solid phase peptide synthesis. Furthermore, the disulfide moiety is cleaved in essentially quantitative yield by conditions (*i.e.* DTT in buffer) that are compatible with standard enzyme assays, including the ELISA-based screen for PTP1B (see below). The Tyr(P) was attached to the amine termini of cystamine as the starting building block. The resin was then split into equal portions for the separate coupling of the linkers **4–26**. The resin from each linker-based reaction was subsequently distributed in 5.0-mg quantities into 8 wells of a single row of 96-well microplates. The terminal diversity elements **A–H** were then incorporated into the library. The resulting resin-linked library members **2** were extensively washed and then subsequently cleaved with 10 mM DTT in 500 μl of 50 mM Tris buffer (pH 8.0) for 3 h. The solution phase was vacuum-filtered into a 96-well receiving plate to afford the spatially discrete library of **3** at a concentration of 0.1 mM (assuming complete conversion for each member). Several library members were resynthesized on a larger scale using the same procedure in high yield and purity (about 90%), as assessed by HPLC and MALDI-TOF MS analysis.

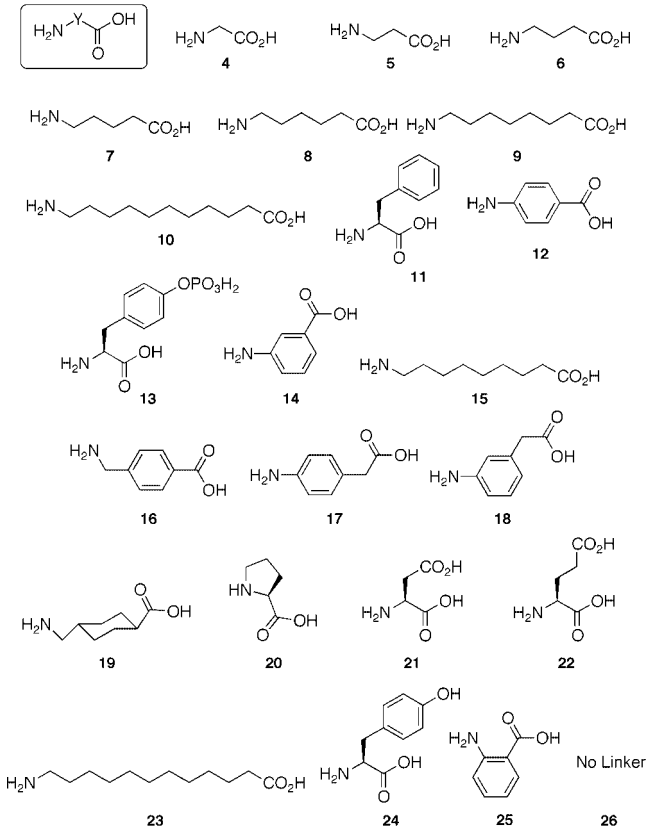

FIG. 2. **Linkers used to connect the N-terminal diversity elements and Tyr(P).** In the case of **26**, the terminal elements are directly linked to Tyr(P).

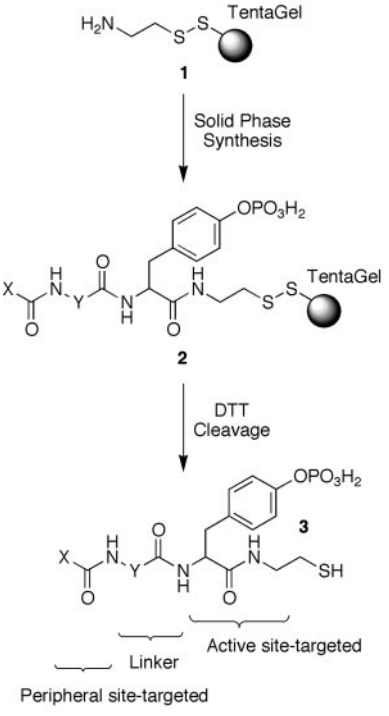

SCHEME I. **Parallel synthesis of a library of compounds targeting both the active site and a unique adjacent site of PTP1B.**

Assay Development—The members of the synthetic library are aryl phosphates and therefore can potentially serve as PTPase substrates. One can identify efficient PTPase substrates by phosphatase activity-based assay (24, 42). However, the most efficient substrate, characterized by the highest k_{cat}/K_m value, does not necessarily possess the highest affinity for the enzyme. Our goal was to identify high affinity PTP1B-binding ligands that can be subsequently converted into non-hydrolyzable analogs as PTP1B inhibitors. Thus we required an affinity-based assay that could easily be adopted for high-throughput screening of a moderate size library of compounds. To this end, we developed an ELISA to screen for high affinity PTP1B substrates that avoids phosphate hydrolysis of library members by PTP1B. This assay requires the use of a catalytically deficient mutant PTP1B that retains the wild type binding affinity. We have previously shown that the active site Cys to Ser PTPase mutant has no measurable phosphatase activity (43) and that the PTP1B/C215S mutant exhibits similar affinity for substrates as the wild-type enzyme (44). We have also shown that the hexameric Tyr(P)-containing peptide DADEpYL-amide is a high affinity PTP1B substrate (41, 44). We prepared the biotinyl-caproic acid-DADEpYL-NH_2 peptide and found that it displayed kinetic parameters similar to those reported for the DADEpYL-NH_2 peptide with the wild-type PTP1B (data not shown). Thus, in this assay the binding affinity of the library members was assessed by their ability to compete with the biotinylated phosphopeptide for binding to PTP1B/C215S.

In the ELISA-based assay (for details, see "Materials and Methods"), Neutravidin (or streptavidin)-coated 96-well microtiter plates were first treated with 10 nM biotinyl-caproic acid-DADEpYL-NH_2 peptide. The plates were then blocked with a solution containing 2% BSA and 0.2% Tween 20 rinsed with a buffer solution. Subsequently, members of the synthetic library (250 nM), individually incubated with GST-PTP1B/C215S (0.2 nM), were introduced into each well of the biotinyl-caproic acid-DADEpYL-NH_2 peptide treated plates. After extensive washing steps, the amount of GST-PTP1B/C215S bound to the biotinylated peptide was detected by primary polyclonal rabbit anti-GST antibody and secondary horseradish peroxidase-conjugated mouse anti-rabbit IgG antibody.

There are several key points to be noted concerning the ELISA-based assay. First, as the reference ligand (biotinylated DADEpYL-NH_2) is known to bind to the PTP1B/C215S active site (18), compounds that displace the reference ligand from PTP1B/C215S most likely bind to the active site as well. Second, as the catalytically inactive PTP1B/C215S binds ligands with equal potency as the wild-type enzyme, this assay furnishes a true assessment of the PTP1B binding ability of the library members. Third, it is known that the invariant active site Cys residue is essential for PTPase catalytic activity (19). Consequently, PTPases are prone to inactivation by oxidizing reagents, heavy metals, and alkylating compounds. This has presented a serious problem for the PTPase activity-based inhibitor screening projects in which hits are identified based on the ability of the compounds to reduce the PTPase activity. The substitution of the active site Cys by a Ser (*e.g.* PTP1B/C215S) renders the mutant PTPase less sensitive to oxidation and alkylation and thus will likely eliminate "false" positives caused by interactions with the active site Cys that destroy the phosphatase activity. Finally, as the assay is ELISA-based, it can be easily implemented for high-throughput PTPase inhibitor discovery.

Identification of High Affinity PTP1B Substrates—The ELISA-based screening protocol employed library members fixed at a 250 nM concentration and was performed in duplicate. This affinity-based screen allowed us to identify several lead compounds that effectively displace GST-PTP1B/C215S from the biotinylated DADEpYL-NH_2 peptide. Several key points are clear from the results graphically depicted in Fig. 3.

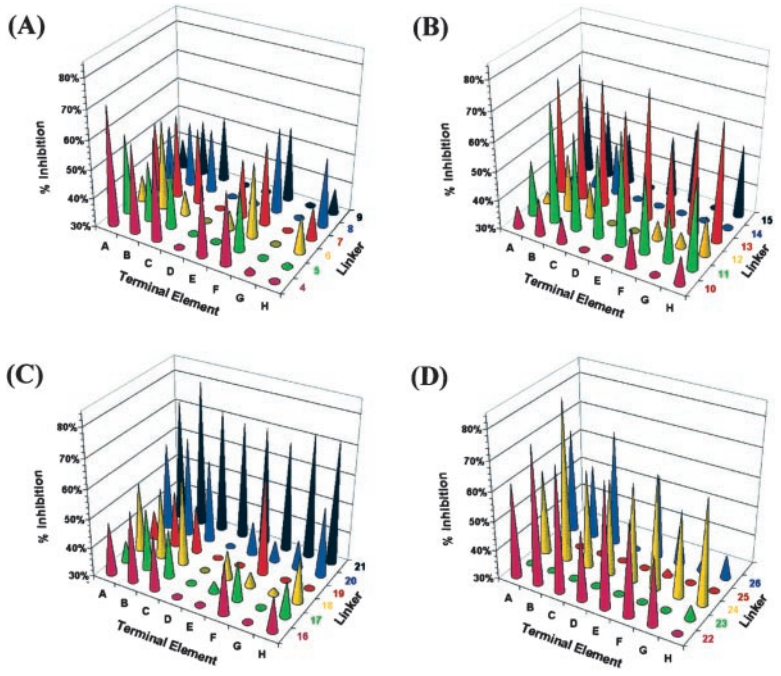

FIG. 3. **Results from the ELISA-based screening of library members at 250 nM concentration.** The potency of the library members for PTP1B is represented by the ability of the compounds to inhibit (expressed as percentage of inhibition) the binding of GST-PTP1B/C215S to the biotinylated DADEpYL-NH_2 peptide immobilized on avidin-coated microtiter plate wells.

First, the naturally occurring amino acids **11**, **13**, **21**, **22**, and **24** serve as the most effective linkers. For example, all the Asp-containing library members (**21A–21H** in Fig. 3*C*) display significant inhibitory potency. Interestingly, these lead linkers are a mix of hydrophobic (**11**, **13**, and **24**) and negatively charged (**13**, **21**, and **22**) residues. The linker position is equivalent to the P-1 position (*i.e.* on the amino side of Tyr(P)) in active site-directed PTPase peptide/protein substrates. We have previously shown that PTP1B undergoes distinct conformational changes that allow it to accommodate either hydrophobic or negatively charged residues at the P-1 site (20). Second, two of the most effective PTP1B ligands (**21B** and **24B**) contain the same N-terminal element, the phosphorylated phenylacetic acid moiety **B**. Finally, PTP1B is clearly quite sensitive to the structural nature of the N-terminal element given the fact that closely related elements (**A** and **C**), which differ by a single methylene group, are less effective than the lead **B**.

To obtain a more accurate assessment of the affinity of these compounds for PTP1B/C215S, we measured the IC_{50} values (compound concentrations that block 50% of the ELISA readout at 450 nm) of the lead compounds (**21B** and **24B**) using **39** as a reference (Fig. 4). For comparison, we also measured the IC_{50} values of compounds **4A** and **4B**, which were less effective than **21B** and **24B** in displacing biotinylated DADEpYL-NH_2 from PTP1B/C215S (Fig. 3). To avoid potential problems associated with the possible oxidation of the thiol tail in the library compounds, we resynthesized compounds **4A**, **21B**, and **24B** without the thiol tail. Table I lists the ratio of the IC_{50} values of the test compounds relative to that of the reference compound **39**. Because **39** is an established competitive inhibitor for PTP1B with a K_i value of 1 μM (39), this IC_{50} ratio should reflect the true affinity of the test compounds for PTP1B (in units of μM). As can be seen from Table I, the presence of the thiol tail in the compounds does not affect the affinity of these compounds for PTP1B/C215S. It can be concluded that compounds **21B** and **24B** display binding affinities significantly higher than that of **39**. In addition, compounds **21B** and **24B** also exhibit higher affinity for PTP1B than that of **4A** and **4B**, consistent with the ELISA results obtained at a single compound concentration (250 nM) (Fig. 3). Finally, although PTP1B can accommodate both Tyr (**24**) and Asp (**21**) at the P-1 position (20, 24), it appears that in the context of the terminal element **B**, the linker Asp (**21**) is slightly favored over Tyr (**24**).

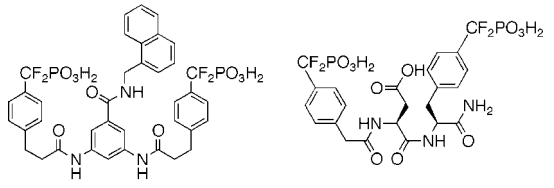

39 40

FIG. 4. **The chemical structures of the reference compound 39 and the nonhydrolyzable analog of 21B, compound 40.**

Determination of K_d Values—The intrinsic fluorescence associated with the N terminus appended coumarin moiety in the 7-hydroxycoumarin-caproic acid-DADEpYL-NH_2 peptide was not significantly altered in the presence of GST-PTP1B/C215S. This property enabled us to determine the dissociation constant for the coumarin derivative via equilibrium dialysis using Slide-A-Lyzer cassettes (see "Materials and Methods"). The K_d value for the binding of 7-hydroxycoumarin-caproic acid-DADEpYL-NH_2 to PTP1B/C215S is 420 ± 20 nM at pH 7.0 and 4 °C. This is similar to the K_d value for the binding of Ac-DADEpYL-NH_2 to PTP1B/C215S determined by isothermal titration calorimetry (800 ± 100 nM) at pH 7.0 and 25 °C. Using the same procedure, the K_d value for the lead compound **21B** can be determined from its ability to displace the 7-hydroxycoumarin-caproic acid-DADEpYL-NH_2 peptide in the dialysis experiment. The K_d value for compound **21B** furnished by equilibrium dialysis is 32 ± 5 nM, which is in agreement with the affinity determined by the ELISA assay (Table I, ~30 nM).

*Acquisition of a Nonhydrolyzable Derivative of **21B**, Compound **40***—As described above, we have identified compound **21B** as the most potent PTP1B-binding ligand from a 184-member spatially discrete library. We next evaluated whether a nonhydrolyzable analog of **21B** can serve as a potent and selective PTP1B inhibitor. Burke and colleagues (45, 46) have shown that the aryl phosphate group in PTPase substrates can be replaced with a hydrolytically resistant difluorophosphonate moiety to produce effective PTPase inhibitors. For example, when phosphonodifluoromethyl phenylalanine (F_2Pmp) re-

TABLE I
Relative Binding Affinity of lead compounds determined by the ELISA assay

Compound	IC_{50}(test)/IC_{50}(reference)
39	1.0
4B	0.70
4A (thiol tail eliminated)	0.79
4A	0.47
24B (thiol tail eliminated)	0.050
24B	0.043
21B (thiol tail eliminated)	0.025
21B	0.035

places the Tyr(P) in the hexapeptide DADEpYL-NH_2, the K_i for the resulting peptide bearing F_2Pmp (200 nM for PTP1B) is over 1000 times more potent than the same peptide containing phosphonomethyl phenylalanine (44, 45, 47). This has been attributed to a direct interaction between the fluorine atoms and PTP1B active site residues (47). Thus we decided to replace the ester oxygens in **21B** with the difluoromethylene group.

The corresponding nonhydrolyzable analog (**40**, Fig. 4) of the high affinity phosphomonoester (**21B**) was prepared via solid phase synthesis using the difluorophosphonate-containing derivatives **32** and **38**. The hydrolytically resistant difluorophosphonate analog (**32**) of **B** was prepared from 4-(bromomethyl)-phenylacetic acid as outlined in Scheme II (39). The unnatural amino acid **38** was synthesized as illustrated in Scheme III. The diphenyloxyazinone intermediate **36** has been previously prepared in five steps from commercially available α-bromo-*p*-toluic acid in an overall 28% yield (31). We developed a somewhat more efficient synthesis (two steps, 42% yield), utilizing the CuBr-mediated coupling of (diethoxyphosphinyl)difluoromethyl]zinc bromide (30) with the aryl iodide **35**. The latter was obtained via the diastereoselective alkylation of the enolate of **34** with the commercially available iodobenzylbromide **33**. The NMR of **36** (T = 100 °C) revealed only a single diastereomer, consistent with the high ee's previously reported for this method (29). Compound **36** was then converted to the desired Fmoc-protected amino acid **38** via hydrogenolysis and subsequent Fmoc protection (31). The standard rotation of **38** ($[\alpha]_D$ = 44°; c = 0.1 in $CHCl_3$) corresponds closely to previously reported values for this compound, confirming that the alkylation of **34** proceeded with high stereoselectivity. Compound **40** was subsequently assembled via the sequential addition of **38**, Fmoc-Asp(O-tBu), and **32** to the Rink amide resin under standard solid phase Fmoc conditions.

*Compound **40** Is the Most Potent and Specific PTP1B Inhibitor Identified to Date*—The effect of the hydrolytically resistant compound **40** on the PTP1B-catalyzed *p*NPP hydrolysis reaction was examined at 25 °C in pH 7.0, 50 mM 3,3-dimethylglutarate buffer, containing 1 mM EDTA and an ionic strength of 0.15 M (for details see "Materials and Methods"). Compound **40** inhibits the PTP1B reaction reversibly, and the mode of inhibition is competitive with respect to the substrate (data not shown). The K_i value for the inhibition of PTP1B by **40** is 2.4 ± 0.2 nM. PTP1B inhibitors with K_i or IC_{50} values in the low nanomolar range have been previously reported (48, 49). However, those measurements were conducted at low, and therefore nonphysiological, ionic strengths. Because of the electrostatic nature of the interactions between the inhibitors and PTP1B active site, it is possible that measurements at low ionic strength may overestimate the binding affinity of these compounds. In support of this, we note that the K_i and K_d values of the hexapeptide DADE(F_2Pmp)L-NH_2 for PTP1B measured under our physiologically relevant conditions (ionic strength of 0.15 M) by enzyme inhibition and isothermal titration calorimetry, are 250 and 240 nM, respectively (44). By contrast,

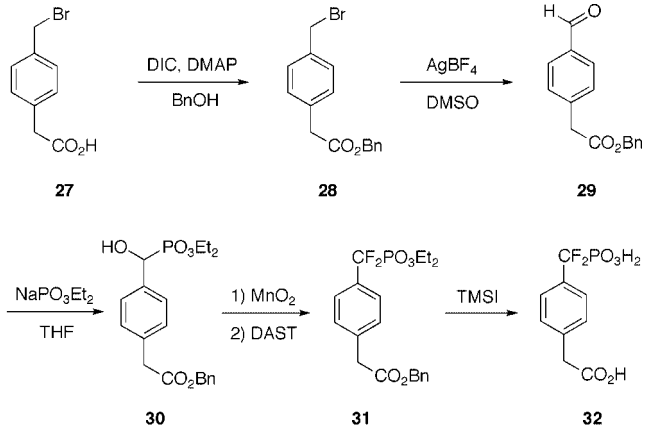

SCHEME II. **Synthesis of the hydrolytically resistant difluorophosphonate analog (32) of B.**

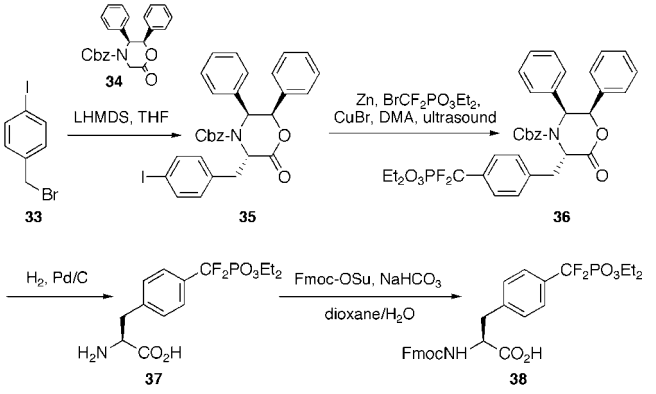

SCHEME III. **Synthesis of the difluorophosphonate-containing unnatural amino acid 38.**

TABLE II
*Selectivity of compound **40** against a panel of protein phosphatases*

Phosphatases	Inhibition potency
PTP1B	K_i = 2.4 nM
TCPTP	K_i = 26 nM
Yersinia PTP	IC_{50} = 1.6 μM
SHP2	IC_{50} = 10 μM
SHP1	IC_{50} = 11 μM
LAR	IC_{50} = 72 μM
HePTP	No inhibition at 10 μM
PTPα	No inhibition at 10 μM
CD45	No inhibition at 10 μM
VHR	No inhibition at 10 μM
MKP3	No inhibition at 10 μM
Cdc25A	No inhibition at 10 μM
Stp1	No inhibition at 10 μM
PP2Cα	No inhibition at 10 μM

the K_i value for the same peptide obtained under previously reported low ionic strength conditions (pH 7.3 in 50 mM Hepes, 5 mM DTT, and 10 μg/ml BSA buffer) is 26 nM (48). In addition, the IC_{50} value of the same peptide under similar low ionic strength conditions (pH 6.3, in 50 mM Bis-Tris, 2 mM EDTA, and 5 mM DTT buffer) is 30 nM (49). Because the ionic strength in both cases is much lower than 0.15 M, it is understandable why a discrepancy exists in the reported PTP1B affinities of the hexapeptide. To further demonstrate the importance of salt concentration on the apparent binding affinity, we also measured the K_i value of compound **40** under identical low salt conditions used by other groups. We found that the K_i of **40** for PTP1B is 0.14 ± 0.01 nM when measured at pH 7.3 in 50 mM Hepes, 5 mM DTT, and 10 μg/ml BSA buffer. Similarly, the K_i of **40** for PTP1B is 0.63 ± 0.09 nM when measured at pH 6.3 in 50 mM Bis-Tris, 2 mM EDTA, and 5 mM DTT buffer. These results highlight the

importance of controlling assay ionic strength to ensure meaningful comparison of inhibitory properties of PTPase ligands. Collectively, our results indicate that compound **40** is the most potent PTP1B inhibitor identified to date.

To determine whether compound **40** is specific for PTP1B, the inhibitory activity of **40** toward a panel of protein phosphatases was evaluated. These included the nonreceptor-like, cytosolic PTPases: the *Yersinia* PTPase. TCPTP, HePTP, SHP1, and SHP2, the receptor-like PTPases (LAR, PTPα, and CD45), the dual specificity phosphatases (VHR, MKP3, and Cdc25A), the low molecular weight phosphatase Stp1, and the Ser/Thr protein phosphatase PP2C. Although a number of potent PTP1B inhibitors have been reported (39, 48–52), achieving selectivity, particularly between PTP1B and TCPTP, has been a considerable challenge. As shown in Table II, compound **40** is highly selective for PTP1B, exhibiting a preference for PTP1B greater than 3 orders of magnitude *versus* nearly all phosphatases examined. More importantly, compound **40** also displays >10-fold selectivity in favor of PTP1B over TCPTP, which is the closest structural homologue of PTP1B (the catalytic domain of PTP1B (residues 1–279) is 69% identical and 85% homologous to that of TCPTP). The high selectivity that is observed for compound **40** without any further optimization is quite impressive, considering the general lack of selectivity that has been observed for inhibitors of the PTPase family members. These results demonstrate that it is possible to achieve both potency and selectivity in PTPase inhibitor development.

Conclusions—In summary, we have described the parallel synthesis of a library of aryl phosphates designed to simultaneously occupy both the PTPase active site and an adjacent nonconserved peripheral site. An affinity-based ELISA screening procedure using the catalytically inactive PTP1B/C215S mutant led to the identification of a potent PTP1B-binding ligand, compound **21B**. Conversion of **21B** into its nonhydrolyzable difluorophosphonate analog **40** produced the most potent and selective PTP1B inhibitor reported to date. This result serves as a proof-of-concept in PTPase inhibitor development, as it demonstrates the feasibility of acquiring potent, yet highly selective, PTPase inhibitory agents. Further biochemical and structural studies are in progress to reveal the molecular basis for the potency and selectivity for compound **40**. PTPase inhibitors, such as **40,** should not only prove useful in dissecting the precise roles played by specific PTPases in signal transduction pathways, but should furnish a molecular foundation upon which therapeutically useful agents will be based.

REFERENCES

1. Zhang, Z.-Y. (2001) *Curr. Opin. Chem. Biol.* **5,** 416–423
2. Ahmad, F., Li, P. M., Meyerovitch, J., and Goldstein, B. J. (1995) *J. Biol. Chem.* **270,** 20503–20508
3. Kenner, K. A., Anyanwu, E., Olefsky, J. M., and Kusari, J. (1996) *J. Biol. Chem.* **271,** 19810–19816
4. Bandyopadhyay, D., Kusari, A., Kenner, K. A., Liu, F., Chernoff, J., Gustafson, T. A., and Kusari, J. (1997) *J. Biol. Chem.* **272,** 1639–1645
5. Wiener, J. R., Kerns, B. J. M., Harvey, E. L., Conaway, M. R., Iglehart, J. D., Berchuck, A., and Bast, R. C., Jr. (1994) *J. Natl. Cancer Inst.* **86,** 372–378
6. Wiener, J. R., Hurteau, J. A., Kerns, B. J., Whitaker, R. S., Conaway, M. R., Berchuck, A., and Bast, R. C., Jr. (1994) *Am. J. Obstet. Gynecol.* **170,** 1177–1183
7. Brown-Shimer, S., Johnson, K. A., Hill, D. E., and Bruskin, A. M. (1992) *Cancer Res.* **52,** 478–482
8. Woodford-Thomas, T. A., Rhodes, J. D., and Dixon, J. E. (1992) *J. Cell Biol.* **117,** 401–414
9. Bjorge, J. D., Pang, A., Fujita, D. J. (2000) *J. Biol. Chem.* **275,** 41439–41446
10. Liu, F., and Chernoff, J. (1997) *Biochem. J.* **327,** 139–145
11. Flint, A. J., Tiganis, T., Barford, D., and Tonks, N. K. (1997) *Proc. Natl. Acad. Sci. U. S. A.* **94,** 1680–1685
12. LaMontagne, K. R., Jr., Flint, A. J., Franza, B. R., Jr., Pandergast, A. M., and Tonks, N. K. (1998) *Mol. Cell. Biol.* **18,** 2965–2975
13. Balsamo, J., Arregui, C., Leung, T., and Lilien, J. (1998) *J. Cell Biol.* **143,** 523–532
14. Liu, F., Hill, D. E., and Chernoff, J. (1996) *J. Biol. Chem.* **271,** 31290–31295
15. Aoki, N., and Matsuda, T. (2000) *J. Biol. Chem.* **275,** 39718–39726
16. Elchebly, M., Payette, P., Michaliszyn, E., Cromlish, W., Collins, S., Loy, A. L., Normandin, D., Cheng, A., Himms-Hagen, J., Chan, C. C., Ramachandran, C., Gresser, M. J., Tremblay, M. L., and Kennedy, B. P. (1999) *Science* **283,** 1544–1548
17. Klaman, L. D., Boss, O., Peroni, O. D., Kim, J. K., Martino, J. L., Zabolotny, J. M., Moghal, N., Lubkin, M., Kim, Y. B., Sharpe, A. H., Stricker-Krongrad, A., Shulman, G. I., Neel, B. G., and Kahn, B. B. (2000) *Mol. Cell. Biol.* **20,** 5479–5489
18. Jia, Z., Barford, D., Flint, A. J., and Tonks, N. K. (1995) *Science* **268,** 1754–1758
19. Zhang, Z.-Y. (1998) *Crit. Rev. Biochem. Mol. Biol.* **33,** 1–52
20. Sarmiento, M., Puius, Y. A., Vetter, S. W., Keng, Y. F., Wu, L., Zhao, Y., Lawrence, D. S., Almo, S. C., and Zhang, Z.-Y. (2000) *Biochemistry* **39,** 8171–8179
21. Lawrence, D. S., and Niu, J. (1998) *Pharmacol. Ther.* **77,** 81–114
22. Cohen, P. (1999) *Curr. Opin. Chem. Biol.* **3,** 459–465
23. Zhang, Z.-Y. (1997) *Curr. Top. Cell. Regul.* **35,** 21–68
24. Vetter, S. W., Keng, Y. F., Lawrence, D. S., and Zhang, Z.-Y. (2000) *J. Biol. Chem.* **275,** 2265–2268
25. Lee, T. R., and Lawrence, D. S. (1999) *J. Med. Chem.* **42,** 784–787
26. Chen, L., Montserat, J., Lawrence, D. S., and Zhang, Z.-Y. (1996) *Biochemistry* **35,** 9349–9354
27. Launikonis, A., Lay, P. A., Mau, A. W.-H., Sargeson, A. M., and Sasse, W. H. F. (1986) *Aust. J. Chem.* **39,** 1053–1062
28. Ganem, B., and Boeckman, R. K., Jr. (1974) *Tetrahedron Lett.* 917–920
29. Williams, R. M., and Im, M.-N. (1991) *J. Am. Chem. Soc.* **113,** 9276–9286
30. Yokomatsu, T., Murano, T., Suemune, K., and Shibuya, S. (1997) *Tetrahedron* **53,** 815–822
31. Solas, D., Hale, R. L., and Patel, D. V. (1996) *J. Org. Chem.* **61,** 1537–1539
32. Smyth, M. S., and Burke, T. R., Jr. (1994) *Tetrahedron Lett.* **35,** 551–554
33. Puius, Y. A., Zhao, Y., Sullivan, M., Lawrence, D. S., Almo, S. C., and Zhang, Z.-Y. (1997) *Proc. Natl. Acad. Sci. U. S. A.* **94,** 13420–13425
34. Zhang, Z.-Y., Clemens, J. C., Schubert, H. L., Stuckey, J. A., Fischer, M., W. F., Hume, D. M., Saper, M. A., and Dixon, J. E. (1992) *J. Biol. Chem.* **267,** 23759–23766
35. Wu, L., and Zhang, Z.-Y. (1996) *Biochemistry* **35,** 5426–5434
36. Zhang, Z.-Y., Wu, L., and Chen, L. (1995) *Biochemistry* **34,** 16088–16096
37. Zhou, B., Wu, L., Shen, K., Zhang, J., Lawrence, D. S., and Zhang, Z.-Y. (2001) *J. Biol. Chem.* **276,** 6506–6515
38. Hao, L., Tiganis, T., Tonks, N. K., and Charbonneau, H. (1997) *J. Biol. Chem.* **272,** 29322–29329
39. Taing, M., Keng, Y. F., Shen, K., Wu, L., Lawrence, D. S., and Zhang, Z.-Y. (1999) *Biochemistry* **38,** 3793–3803
40. Zhang, Z.-Y., Maclean, D., Thieme-Sefler, A. M., McNamara, D., Dobrusin, E. M., Sawyer, T. K., and Dixon, J. E. (1993) *Proc. Natl. Acad. Sci. U. S. A.* **90,** 4446–4450
41. Zhang, Z.-Y., Maclean, D., McNamara, D. J., Sawyer, T. K., and Dixon, J. E. (1994) *Biochemistry* **33,** 2285–2290
42. Montserat, J., Chen, L., Lawrence, D. S., and Zhang, Z.-Y. (1996) *J. Biol. Chem.* **271,** 7868–7872
43. Zhang, Z.-Y., and Wu, L. (1997) *Biochemistry* **36,** 1362–1369
44. Zhang, Y.-L., Yao, Z.-J., Sarmiento, M., Wu, L., Burke, T. R., Jr., and Zhang, Z.-Y. (2000) *J. Biol. Chem.* **275,** 34205–34212
45. Burke, T. R., Jr., Smyth, M., Nomizu, M., Otaka, A., and Roller, P. P. (1993) *J. Org. Chem.* **58,** 1336–1340
46. Burke, T. R., Jr., Kole, H. K., and Roller, P. P. (1994) *Biochem. Biophys. Res. Commun.* **204,** 129–134
47. Chen, L., Wu, L., Otaka, A., Smyth, M. S., Roller, P. P., Burke, T. R., den Hertog, J., and Zhang, Z.-Y. (1995) *Biochem. Biophys. Res. Commun.* **216,** 976–984
48. Huyer, G., Kelly, J., Moffat, J., Zamboni, R., Jia, Z., Gresser, M. J., and Ramachandran, C. (1998) *Anal. Biochem.* **258,** 19–30
49. Desmarais, S., Friesen, R. W., Zamboni, R., and Ramachandran, C. (1999) *Biochem. J.* **337,** 219–223
50. Wrobel, J., Sredy, J., Moxham, C., Dietrich, A., Li, Z., Sawicki, D. R., Seestaller, L., Wu, L., Katz, A., Sullivan, D., Tio, C., and Zhang, Z.-Y. (1999) *J. Med. Chem.* **42,** 3199–3202
51. Iversen, L. F., Andersen, H. S., Branner, S., Mortensen, S. B., Peters, G. H., Norris, K., Olsen, O. H., Jeppesen, C. B., Lundt, B. F., Ripka, W., Moller, K. B., and Moller, N. P. (2000) *J. Biol. Chem.* **275,** 10300–10307
52. Bleasdale, J. E., Ogg, D., Palazuk, B. J., Jacob, C. S., Swanson, M. L., Wang, X. Y., Thompson, D. P., Conradi, R. A., Mathews, W. R., Laborde, A. L., Stuchly, C. W., Heijbel, A., Bergdahl, K., Bannow, C. A., Smith, C. W., Svensson, C., Liljebris, C., Schostarez, H. J., May, P. D., Stevens, F. C., and Larsen, S. D. (2001) *Biochemistry* **40,** 5642–5654